Analytical method to determine the orientation of rigid spin labels in DNA

Andriy Marko,[1,*] Dominik Margraf,[1] Pavol Cekan,[2] Snorri Th. Sigurdsson,[2] Olav Schiemann,[3] and Thomas F. Prisner[1]

[1]*Institute of Physical and Theoretical Chemistry, J. W. Goethe University, Max-von-Laue-Str. 7, D-60438 Frankfurt, Germany*
[2]*Science Institute, University of Iceland, Dunhaga 3, 107 Reykjavik, Iceland*
[3]*Centre for Biomolecular sciences, Centre of Magnetic Resonance, University of St. Andrews, North Haugh,*
KY169ST St. Andrews, United Kingdom

We demonstrate the ability of pulsed electron double resonance (PELDOR) experiments to determine the orientation of spin labels in biological macromolecules. Thus, the distance information usually obtained from PELDOR data can be complemented by the mutual orientation of macromolecular domains. A method to determine the angle β between the spin label normal and the interspin axis is proposed and analyzed mathematically. The obtained analytical expression allows extraction of angles β without a fitting procedure if these angles are equal for both nitroxide of biradical. The method was applied to the experimental data gathered on ten spin-labeled DNA samples. The angles estimated from the PELDOR data are in excellent agreement with literature values.

I. INTRODUCTION

Determination of structure and dynamics of biological macromolecules is essential regarding their functional characterization. X-ray crystallography is a classical method for structural characterization at atomic resolution. However, crystallization of biological samples is a complicated process, which does not necessarily conserve them in their functional state. High-resolution NMR spectroscopy is a technique which can reveal structure as well as dynamics of biomolecules under native conditions, but its application is restricted to system size of about 50 kDa. To determine distances and conformational changes in the nm range in macromolecules pulsed electron-electron double resonance (PELDOR) [1–5] as well as fluorescence resonance energy transfer (FRET) [6] have been successfully employed. Both methods have no restrictions with regard to the size of the molecules. Similarly to FRET, which utilizes the electric dipole-dipole interaction between two chromophores, PELDOR uses the magnetic dipole-dipole interaction between paramagnetic centers that depends on the distance $r=|\mathbf{r}|$ between them and on the angle Θ between the static magnetic field B_0 and the interspin vector $\mathbf{r}$.

In typical applications of PELDOR to proteins, DNA or RNA molecules, nitroxide spin labels are used as paramagnetic markers [7–14]. In many studies the attached spin labels were flexible enough to exhibit an almost random mutual orientation. Under such conditions the PELDOR signal is solely expressed via the distance distribution between the two spin labels, $f(r)$. Vice versa, the function $f(r)$ can be deducted from PELDOR time traces, e.g., via Tikhonov regularization [15–18]. The description of the PELDOR signal becomes more complicated for rigidly embedded paramagnetic centers, as native cofactors, or for spin labels with restricted flexibility [19–21]. In this case the time traces contain additional information about the mutual orientation of

the spin labels with respect to each other and to the interspin vector $\mathbf{r}$. Recent studies revealed the possibility to extract this orientational information from PELDOR experiments by a quantitative simulation or fitting procedures which explicitly include an appropriate model of such conformational restrictions. Resolving the g-tensor of the tyrosyl radicals in a ribonucleotide reductase dimer at high enough magnetic field, the mutual orientation between the two monomers could be determined [22–24]. The method has also been applied to binitroxide model compounds to determine additionally geometrical constraints [25–28]. Previously, we have described rigid nitroxide Ç (see Figs. 1 and 3), which can be incorporated site specifically into duplex DNA [10,29], and have shown that information about the relative orientation of such spin labels can be determined by PELDOR [28]. In all these cases, the PELDOR data were simulated by assuming a reasonable geometry and flexibility of the biradical.

The main goal of this publication is to express analytically the parameters characterizing the geometry of a pair of rigid spin labels Ç, directly from the experimental PELDOR time traces. Indeed, we show that this problem can be exactly solved in special cases, when, for example, both spin label planes are parallel. This method was tested on double helical DNA molecules with two rigid spin labels [28]. The nitroxide radicals are covalently attached to the cytosine nucleobases on complementary strands of the DNA double helix (see Fig. 1). The planes of the nitroxide radicals are coplanar with the planes of the base pairs. As a consequence, the plane normals, which coincide with the principle axis A_{zz} of the hyperfine interaction tensor of the unpaired electron with the ^{14}N nucleus, are parallel to each other. The angle β between the A_{zz} axis and the vector $\mathbf{r}$ connecting the two unpaired electron spins will be the same for both nitroxides in the studied DNA molecules. Our procedure allowed us to determine β analytically from PELDOR time traces with variable probe frequencies.

II. METHODS

To elucidate our ansatz we will take a closer look at the factors causing the modulation of the PELDOR signal. The

*marko@prisner.de
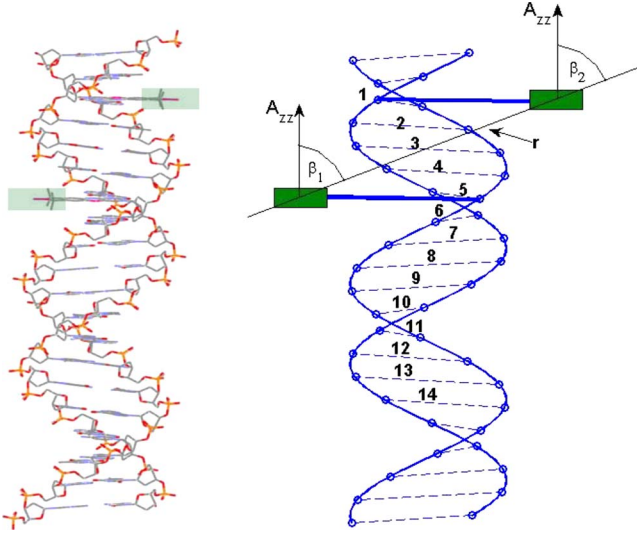
FIG. 1. (Color online) Structure (left) and schematic presentation (right) of a double labeled DNA molecule. The spin labels (marked by green rectangles) are attached to the base pairs with the numbers 1 and 5. In our nomenclature this system is noted as DNA(1,5) inherited from the general expression DNA (m,n), where m and n are the positions of the first and of the second spin labels, respectively. A_{zz} is the principle axis of hyperfine interaction tensor, which coincides with the nitroxide plane normal. Since the planes of the spin labels are coplanar with the base pairs, the angles β_1 and β_2 are approximately equal.

frequencies of the two allowed transitions between the energy levels of two interacting electron spins is given by the expression

$$\omega_{dd}(r,\Theta) = \pm D(1 - 3\cos^2\Theta)/r^3, \quad (1)$$

where $D = \mu_0 (g_e \mu_B)^2/(4\pi\hbar) = 2\pi \times 52.04$ MHz nm^3 is the dipolar interaction constant. For a weakly anisotropic g-tensor it is expressed through the following fundamental physical constants: the magnetic susceptibility of vacuum, μ_0, the g-value of free electron, g_e, the Bohr magneton, μ_B, and Planck's constant $\hbar$. In a powder, all orientations of the interspin vector are equally probable. For a system without orientation selection the spectrum consist of a superposition of doublets weighted according to the probability, $p(\Theta)d\Theta$, that the polar angle is found in the range $[\Theta, \Theta + d\Theta]$. This probability is given by the quotient of the solid angle defined by this polar angle range and the full solid angle $p(\Theta)d\Theta = 2\pi \sin\Theta d\Theta/(4\pi) = |d\cos\Theta|/2$. If the polar angle is expressed via the frequency, i.e., $p(\Theta)d\Theta = g(\omega)d\omega$, then we obtain the spectral density function $g(\omega)$ known as the Pake pattern. For a system with orientation selection the superposition of doublets should be additionally weighted with a function $\lambda(\Theta)$, which shows the contribution of biradicals with the orientation Θ to the total PELDOR signal [27]. The shape of the function λ depends on the position of the probe and pump pulses because the selection of certain nitroxide orientations inevitably leads to the selection of certain polar angles of rigid biradicals. For example, a probe pulse with the frequency ω_A excites nitroxide radicals with the A_{zz} axis lying on a cone with an opening $\phi(\omega_A)$ around the static
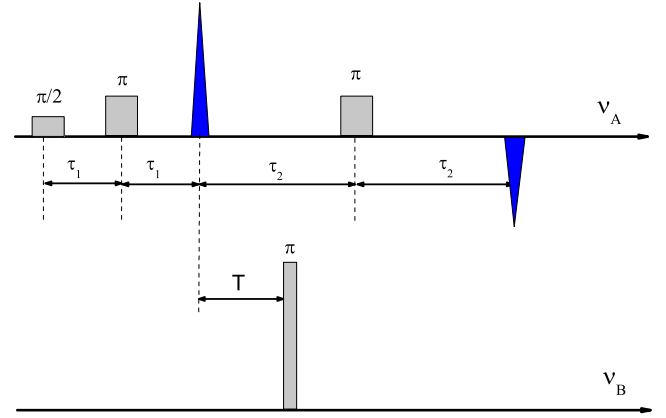
FIG. 2. (Color online) Pulse sequence for four-pulse PELDOR. ν_A and ν_B are probe and pump frequencies, respectively. τ_1 is the delay between the first and the second microwave pulses. τ_2 is the time between the first echo and the third probe pulse. T is the delay between the first echo and the pump pulse.

magnetic field $\boldsymbol{B}_0$. If the frequency ω_A is chosen in a way that the angle $\phi(\omega_A)$ is equal to the angle β defined for our DNA model systems, then it will lead to a strong selection of biradicals with interspin axes $\boldsymbol{r}$ parallel to the static magnetic field B_0. Therefore, one can try to estimate the angle β by detecting the probe pulse frequency ω_A^{max} giving rise to a high intensity of the Pake pattern edges.

To determine orientation intensities of electron spin-spin interaction or the shape of Pake pattern for different probe pulse positions, the dead-time-free PELDOR experiment [30] (see Fig. 2) with a fixed pump frequency and varied probe frequencies across the nitroxide X-band spectrum is used. In a simple case of electron spin pairs with uncorrelated Larmor frequencies, PELDOR can be explained in the following way. The three pulses at the probe frequency ν_A form an echo from the spins on resonance (called A spins). Application of the pump pulses at the frequency ν_B invert the resonant with this frequency spins (called B spins), which can be spatially close to the probed A spins. Due to spin-spin interaction the Larmor frequency of the A spins is shifted by ω_{dd}, leading to a phase shift $\omega_{dd}T$ of the observed signal and modulation of the refocused Hahn echo. Here T is the delay of pumping pulse. The observed signal consists of two parts. One of them is constant in time and proportional to the probability $1-p$ that B spin was not flipped by the pump pulse and the second part is proportional to the probability p of the B spin flip and is modulated in time, i.e., $p\cos(\omega_{dd}T)$. In a more complicated case, when the Larmor frequencies of two electron spins are correlated or when the mutual orientation of the two radicals is rigidly fixed, the description of PELDOR signals must take into account radicals orientations (see next section).

III. THEORY

A. Description of the PELDOR signal

The geometrical structure of the studied double labeled DNA molecules can be conveniently described using an ap-
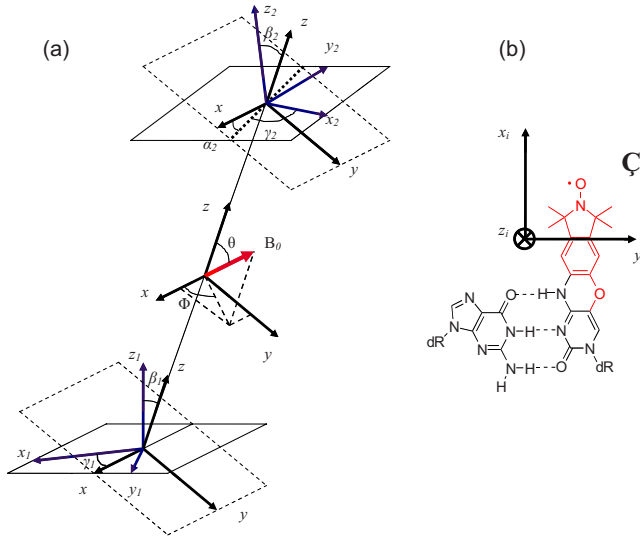
FIG. 3. (Color online) (a) Three coordinate systems for the description PELDOR signal of a rigid biradical. $\{x_1,y_1,z_1\}$ and $\{x_2,y_2,z_2\}$ frames correspond to the principal axes of the first and the second nitroxide, respectively. $\{x,y,z\}$ has the z axis coinciding with the interspin axis r and x axis is perpendicular to both vectors z and z_1. The transition from $\{x,y,z\}$ to $\{x_i,y_i,z_i\}$ is done in three subsequent steps via two intermediate systems $\{x_i',y_i',z_i'\}$ and $\{x_i'',y_i'',z_i''\}$ (not shown here). The system $\{x_i',y_i',z_i'\}$ is the result of a rotation of $\{x,y,z\}$ about the z axis through the angle α_i. The system $\{x_i'',y_i'',z_i''\}$ is obtained after a rotation of $\{x_i',y_i',z_i'\}$ about the x_i' axis through the angle β_i. To obtain $\{x_i,y_i,z_i\}$ the frame $\{x_i'',y_i'',z_i''\}$ is rotated about the z_i'' axis through the angle γ_i. Within this definition of Euler angles the angle α_1 is always equal to zero. Angles Θ and Φ describe orientation of the external magnetic field in $\{x,y,z\}$ frame. (b) Rigid nitroxide Ç base-paired with guanine.

propriate coordinate frame as depicted in Fig. 3. The first and the second nitroxide radicals are associated with their principal axis frames $\{x_1,y_1,z_1\}$ and $\{x_2,y_2,z_2\}$, respectively, which are defined by choosing the x axis parallel to the NO bond and the z axis parallel to the plane normal of the radical. Furthermore, we introduce the dipolar coordinate system with the unit vectors $\{x,y,z\}$, whose z axis coincides with the interspin vector r and x axis is oriented orthogonally to the plane of two vectors z and z_1, i.e., $x=z\times z_1$. In this coordinate system the orientation of the external magnetic field B_0 is given by the polar angle Θ and the azimuth angle Φ and the orientation of the two radicals is characterized by the Euler angles $(\alpha_1,\beta_1,\gamma_1)\equiv o_1$ and $(\alpha_2,\beta_2,\gamma_2)\equiv o_2$. Since the angle α_1 is equal to zero for any mutual orientation of nitroxides (see Fig. 3), the geometry of biradical is virtually characterized by five angles $\beta_1,\gamma_1,\alpha_2,\beta_2,\gamma_2$. Using the coordinate systems introduced above, the modulation of the refocused Hahn echo magnitude can be described by the expression

$$v(T,\omega_A,\omega_B,) = v_0(\omega_A) + \int_0^{\pi/2} d\Theta\ \sin\Theta u(\omega_A,\omega_B,\Theta,o_1,o_2)$$

$$\times[\cos(\omega_{dd}(r,\Theta)T)-1]. \qquad (2)$$

Here, $v_0(\omega_A)$ is the refocused Hahn-echo signal with frequency ω_A in the absence of the pump pulse. The function

$u(\omega_A,\omega_B,\Theta,o_1,o_2)$ reflects the signal intensity modulation, which is proportional to the magnetization of the A spin and multiplied by the flip probability of the B spin. Equation (2) describes the PELDOR signal by assuming a single conformation of the molecule. However, due to thermal motion the studied molecules can be in different conformations [25,26] resulting in an ensemble of $i=1,\ldots,N$ molecular structures with various dipolar distances r_i and spin label orientations $o^{(i)}$. The total PELDOR signal $V(T,\nu)$ is given as an average over this ensemble

$$V(T,\omega_A,\omega_B) = V_0(\omega_A)$$

$$+ \sum_{i=1}^{N} \int_0^{\pi/2} d\Theta\ \sin\Theta u(\omega_A,\omega_B,\Theta,o_1^{(i)},o_2^{(i)})$$

$$\times[\cos(\omega_{dd}(r_i,\Theta)T)-1]. \qquad (3)$$

Equation (3) is too complicated in order to express the biradical conformation characterizing Euler angles o_1 and o_2 via the signal function $V(T,\omega_A,\omega_B)$. It can be simplified if the conformational average $\langle\ldots\rangle=\frac{1}{N}\Sigma_{i=1}^N(\ldots)$ in Eq. (3) is approximated by the product of two averages, i.e.,

$$\langle u[\omega_A,\omega_B,\Theta,o_1^{(i)},o_2^{(i)}]\cos[\omega_{dd}(r_i,\Theta)T]\rangle$$

$$= \langle u[\omega_A,\omega_B,\Theta,o_1^{(i)},o_2^{(i)}]\rangle\langle\cos[\omega_{dd}(r_i,\Theta)T]\rangle. \qquad (4)$$

This approximation is obviously true if the function $u(\omega_A,\omega_B,\Theta,o_1^{(i)},o_2^{(i)})$ does not depend on the index i of biradical that is realized for the systems with the fixed mutual orientation of the spin labels. The decomposition (4) is justified if the fluctuations of spin labels distances r are only weakly correlated with the fluctuation of Euler angles o_1 and o_2 [27]. Introducing $z=\cos\Theta$, the above factorization allows us to write the normalized PELDOR signal $S(T,\omega_A,\omega_B)$ $=V(T,\omega_A,\omega_B)/V_0(\omega_A)$ in the form of a Fredholm integral equation of the first kind [15]:

$$S(T,\nu) = 1 + \int_0^1 \lambda(z,\omega_A,\omega_B)K(z,T)dz, \qquad (5)$$

with the kernel function

$$K(z,T) = \langle\cos[\omega_{dd}(r_i,\Theta)T]\rangle - 1, \qquad (6)$$

and the orientation intensity function

$$\lambda(z,\omega_A,\omega_B) = \frac{1}{v_0(\omega_A)}\langle u(\omega_A,\omega_B,\Theta,o_1^{(i)},o_2^{(i)})\rangle. \qquad (7)$$

A detailed analysis of the function $\lambda(z,\omega_A,\omega_B)$ is done in the next section. Here, we just note that the function $\lambda(z,\omega_A,\omega_B)$ is constant if orientation selection does not occur in the system. The function $\lambda(z,\omega_A,\omega_B)$ allows us to express the PELDOR signal at long times when all oscillations are damped, in a simple way

$$S(\infty,\omega_A,\omega_B) = 1 - \int_0^1 \lambda(z,\omega_A,\omega_B,)dz. \qquad (8)$$

The orientation intensity function $\lambda(z,\omega_A,\omega_B,)$ can be estimated numerically solving Eq. (5) for a known kernel function $K(z,T)$ [27]. This method is used later on in order to

analyze the experimental data. An alternative way to approximately estimate the values of the function $\lambda(z,\omega_A,\omega_B)$ for $z \to 1$ is to find the Fourier transformation of the asymptotic value subtracted PELDOR signal, i.e., to find $g(\omega) = 1/(2\pi) \int_{-\infty}^{\infty} [S(T,\omega_A,\omega_B) - S(\infty,\omega_A,\omega_B)] \exp(i\omega T) dT$. Using the Fourier representation of the δ-function $\delta(k) = 1/(2\pi) \int_{-\infty}^{\infty} \exp(ikx) dx$ [Eqs. (5) and (8)], we get

$$g(\omega) = \sum_i^N \int_0^1 \lambda(z,\omega_A,\omega_B) \{ \delta[\omega - \omega_{dd}(r_i,z)]$$
$$+ \delta[\omega + \omega_{dd}(r_i,z)] \} dz. \qquad (9)$$

Integration over z result in

$$g(\omega) = \sum_i^N [g_+^{(i)}(\omega) + g_-^{(i)}(\omega)], \qquad (10)$$

with

$$g_+^{(i)}(\omega)$$
$$= \begin{cases} \dfrac{\lambda[\sqrt{(\omega_{\perp i} + \omega)/(3\omega_{\perp i})}, \omega_A, \omega_B]}{2\sqrt{3\omega_{\perp i}(\omega_{\perp i} + \omega)}} & -\omega_{\perp i} < \omega \le 2\omega_{\perp i} \\ 0 & \text{otherwise} \end{cases}$$
$$(11)$$

and

$$g_-^{(i)}(\omega)$$
$$= \begin{cases} \dfrac{\lambda[\sqrt{(\omega_{\perp i} - \omega)/(3\omega_{\perp i})}, \omega_A, \omega_B]}{2\sqrt{3\omega_{\perp i}(\omega_{\perp i} - \omega)}} & -2\omega_{\perp i} \le \omega < \omega_{\perp i} \\ 0 & \text{otherwise.} \end{cases}$$
$$(12)$$

Here $\omega_{\perp i} = D/r_i^3$ is the single dipolar frequency of the ith biradical. Its ensemble averaged value is denoted as $\langle \omega_\perp \rangle$. The spectral density g is an even function, $g(\omega) = g(-\omega)$. Equations (10)–(12) allow us to estimate the value of the orientation intensity function at $\Theta = 0$ or $\cos \Theta = 1$ from g,

$$\lambda(1,\omega_A,\omega_B) \approx g(2\langle\omega_\perp\rangle)6\langle\omega_\perp\rangle = g(-2\langle\omega_\perp\rangle)6\langle\omega_\perp\rangle. \qquad (13)$$

The last expression means that the value of the orientation intensity function at the point $\Theta = 0$ is proportional to the value of the Pake pattern at its edges. Therefore, if we are interested in the ω_A dependence on the function $\lambda(1,\omega_A,\omega_B)$, it can be obtained from the Fourier transformation of the PELDOR time traces with different offsets between the probe and pump pulses.

B. Analysis of the orientation intensity function

The resonance frequency ω_r of the two electron spins is determined by (i) the Zeeman interaction with the external magnetic field, (ii) the hyperfine interaction with the ^{14}N nucleus, and (iii) local field fluctuations leading to inhomogeneous line broadening δb. This yields [3,19,20]

$$\omega_r(\Theta,\Phi,\boldsymbol{o},m) = \gamma_0 [B_0 g_{\text{eff}}(\Theta,\Phi,\boldsymbol{o})/g_e + m A_{\text{eff}}(\Theta,\Phi,\boldsymbol{o}) + \delta b], \qquad (14)$$

where $\boldsymbol{o} = \boldsymbol{o}_1, \boldsymbol{o}_2$ represents the Euler angles of spin 1 and 2, respectively, γ_0 denotes the gyromagnetic ratio of electron, and the quantum number $m = -1, 0, 1$ accounts for the state of the nuclear spin. Functions $g_{\text{eff}}(\Theta,\Phi,\boldsymbol{o})$ and $A_{\text{eff}}(\Theta,\Phi,\boldsymbol{o})$ are effective values of the g tensor and hyperfine interaction tensor A in the dipolar coordinate system, respectively. They can be calculated from [3] the square root of

$$T_{\text{eff}}^2(\Theta,\Phi,\boldsymbol{o}) = T_{xx}^2 + (T_{yy}^2 - T_{xx}^2)[\sin\Theta \sin\gamma \cos(\alpha - \Phi)$$
$$+ \sin\Theta \cos\gamma \sin(\alpha - \Phi)\cos\beta$$
$$+ \cos\Theta \cos\gamma \sin\beta]^2 + (T_{zz}^2 - T_{xx}^2)$$
$$\times [\sin\Theta \sin\beta \sin(\alpha - \Phi) + \cos\Theta \cos\beta]^2, \qquad (15)$$

where T can be either the g tensor or the A tensor. The function T_{eff} is symmetric with respect to the origin of the coordinate system, i.e., $T_{\text{eff}}(\Theta,\Phi,\boldsymbol{o}) = T_{\text{eff}}(\pi - \Theta, \pi + \Phi, \boldsymbol{o})$. For $\boldsymbol{o} = 0$, Eq. (15) simplifies to $T_{\text{eff}}^2(\Theta,\Phi,0) = T_{xx}^2 \sin^2\Theta \cos^2\Phi + T_{yy}^2 \sin^2\Theta \sin^2\Phi + T_{zz}^2 \cos^2\Theta$.

We first introduce the electron spin Rabi frequency Ω_i, which is caused by microwave excitation with frequency ω_i and field strength B_{1i}, i.e.,

$$\Omega_i^2(k) = \gamma_0^2 B_{1i}^2 + [(\omega_i - \omega_r(\Theta,\Phi,\boldsymbol{o}_k,m_k)]^2, \qquad (16)$$

where $i = A, B$ indicates the probe and pump pulses, respectively. After the application of three rectangular detection pulses, the x component of the spin echo magnetization is equal to [19,20,31,32]

$$m_x(\Omega_A) = \frac{1}{4} \left[\frac{\gamma_0 B_{1A}}{\Omega_A} \right]^5 \sin(\Omega_A t_A)[1 - \cos(\Omega_A t_A')]^2. \qquad (17)$$

To calculate the total transversal magnetization, the magnetization m_x of the A spin is weighted by the flip probability of the B-spin. This probability is given by [19,20,32]

$$p(\Omega_B) = \frac{\gamma_0^2 B_{1B}^2}{2\Omega_B^2}[1 - \cos(\Omega_B t_B)], \qquad (18)$$

for the rectangular pump pulse of a length t_B. Hence, the total transversal magnetization for both unpaired spins can be written as

$$\xi(\omega_A,\omega_B,1,2) = m_x[\Omega_A(1)] p[\Omega_B(2)] + m_x[\Omega_A(2)] p[\Omega_B(1)]. \qquad (19)$$

The experimentally measured magnetization is given as an average (i) over all ^{14}N nuclear spin states m_1 and m_2, (ii) over the azimuthal angle Φ, and (iii) over the inhomogeneous line-shape broadening δb (which is assumed to be Gaussian). This leads to the desired expression for the orientation intensity function

$$u(\omega_A,\omega_B,\Theta,\boldsymbol{o}_1,\boldsymbol{o}_2) = \sum_{m_1,m_2} \overline{\xi(\omega_A,\omega_B,1,2)}_{\Phi,\delta b_1,\delta b_2}. \qquad (20)$$

A similar expression can be derived for the refocused Hahn echo magnetization $v_0(\nu)$ in the absence of the pump pulse.

Inserting expressions (16)–(19) into the Eq. (20), the function $u(\omega_A, \omega_B, \Theta, o_1, o_2)$ determining the PELDOR signal can be calculated. In general it has a complicated form. Therefore, it is difficult to analytically express the angles o_1 and o_2 via the values of the function u. However, taking into account our experimental conditions and symmetry of the studied systems, expression (20) can be simplified for $\Theta = 0$. To a good approximation the g tensor and the hyperfine interaction tensor can be considered as axially symmetric in X band. For $\Theta = 0$ it means that the resonance frequency of radical [see Eqs. (14) and (15)] does not depend on the azimuth angle Φ and the averaging over this angle can be omitted in Eq. (20). In our experiments the probe pulses at the frequency ω_A excite electronic transition with the nuclear spin state 1, therefore the double summation in Eq. (20) is reduced to a single one. Taking into account the above remarks, Eqs. (19) and (20) simplify to

$$u(\omega_A, \omega_B, \Theta, o_1, o_2) = \overline{m_x[\widetilde{\Omega}_A(1)]}_{\delta b_1} \sum_{m_2} \overline{p[\Omega_B(2)]}_{\delta b_2}$$
$$+ \overline{m_x[\widetilde{\Omega}_A(2)]}_{\delta b_2} \sum_{m_1} \overline{p[\Omega_B(1)]}_{\delta b_1}. \tag{21}$$

Here $\widetilde{\Omega}_A(1)$ and $\widetilde{\Omega}_A(2)$ are the values of Rabi frequencies of the first and the second nitroxide, respectively, calculated from Eq. (16) for $\Theta = 0$ and nuclear spin state 1. Furthermore we will average the transversal magnetization component over the inhomogeneous line width. For this reason we will represent the Rabi frequency in the next form

$$\widetilde{\Omega}_i^2(k) = \gamma_0^2 \{B_{1i}^2 + [\Delta_i(\beta_k) - \delta b_k]^2\}, \tag{22}$$

where $\Delta_i(\beta_k)$ is defined by the equation $\Delta_i(\beta_k) = \omega_i / \gamma_0 - B_0 g_{\text{eff}}(0,0,o_k)/g_e - A_{\text{eff}}(0,0,o_k)$, with $o_k = (0, \beta_k, 0)$. Using this equation the function $m_x(\widetilde{\Omega}_A(k)_{\delta b_k}$ can be rewritten as a new function $\widetilde{m}_x$ of the variable $\Delta_A(\beta_k)$. For the Gaussian inhomogeneous line broadening we end up with

$$\widetilde{m}_x[\Delta_A(\beta_k)] \equiv \overline{m_x[\widetilde{\Omega}_A(k)]}_{\delta b_k} = \int_{-\infty}^{\infty} m_x[\widetilde{\Omega}_A(k)] \frac{\exp\left(-\frac{\delta b_k^2}{2\sigma^2}\right)}{\sqrt{2\pi\sigma^2}} d\delta b_k. \tag{23}$$

Here σ is the inhomogeneous line width. If σ is much smaller than the B_{1A} field then $\widetilde{m}_x[\Delta_A(\beta_k)] = m_x[\gamma_0 \sqrt{B_{1A}^2 + \Delta_A^2(\beta_k)}]$ and the function $\widetilde{m}_x$ reaches its maximum value equal to 1 at the point $\Delta_A(\beta_k) = 0$. In the case when the value of σ is larger than the magnitude of the B_{1A} field, then $\widetilde{m}_x[\Delta_A(\beta_k)]$ can be approximated by the following expression:

$$\widetilde{m}_x(\Delta_A(\beta_k)) = M(B_{1A}, \sigma) \frac{\exp\left(-\frac{\Delta_A^2(\beta_k)}{2\sigma^2}\right)}{\sqrt{2\pi\sigma^2}}, \tag{24}$$

where

$$M(B_{1A}, \sigma) = \exp\left(\frac{B_{1A}^2}{2\sigma^2}\right) \int_{\gamma_e B_{1A}}^{\infty} \frac{m_x(x)x}{\gamma_e \sqrt{x^2 - \gamma_e^2 B_{1A}^2}}$$
$$\times \exp\left(-\frac{x^2}{2\gamma_e^2\sigma^2}\right) dx. \tag{25}$$

We note that in Eq. (24) the magnetization $\widetilde{m}_x$ is written as a product of a Gaussian function, which depends on the geometry of the biradical, and the function M, which does not depend on the mutual orientation of nitroxides but depends on the probe pulse parameters.

Since DNA base pairs as well as the nitroxide Ç planes can be considered as parallel, we can assume that the ensemble averaged values of the angles β_1 and β_2 are equal $\langle\beta_1\rangle = \langle\beta_2\rangle = \beta$. The deviation of these angles from the averaged position is denoted as $\Delta\beta_k = \beta_k - \beta$ with $k = 1, 2$. For the small variation in the angle β_k, the function $\Delta_A(\beta_k)$ can be presented in the form of Tailor series $\Delta_A(\beta_k) \approx \Delta_A(\beta) + \Delta_A'(\beta)\Delta\beta_k$. If the angles β_k are normally distributed around a central value β with variance $\langle\Delta\beta^2\rangle$, then we can also perform an ensemble average of expression (24):

$$\int_{-\infty}^{\infty} \widetilde{m}_x(\Delta_A(\beta) + \Delta_A'(\beta)\Delta\beta_k) \frac{\exp\left(-\frac{\Delta\beta_k^2}{2\langle\Delta\beta^2\rangle}\right)}{\sqrt{2\pi\langle\Delta\beta^2\rangle}} d\Delta\beta_k$$
$$= \frac{M(B_{1A}, \sigma)}{\sqrt{2\pi\sigma^{*2}}} \exp\left(-\frac{\Delta_A^2(\beta)}{2\sigma^{*2}}\right). \tag{26}$$

Here, σ^* can be considered as an effective inhomogeneous line width, which is determined by the expression $\sigma^{*2} = \sigma^2 + \Delta_A'^2(\beta)\langle\Delta\beta^2\rangle$. After ensemble averaging both functions $m_x(\widetilde{\Omega}_A(1))_{\delta b_1}$ and $m_x(\widetilde{\Omega}_A(2))_{\delta b_2}$ become equal. This allows us to write expression (21) in the following form:

$$\langle u(\omega_A, \omega_B, 0, o_1^{(i)}, o_2^{(i)})\rangle = \langle P\rangle \frac{M(B_{1A}, \sigma)}{\sqrt{2\pi\sigma^{*2}}} \exp\left(-\frac{\Delta_A^2(\beta)}{2\sigma^{*2}}\right), \tag{27}$$

where $\langle P\rangle$ is the ensemble average of expression

$$P = \sum_{m_2} \overline{p(\Omega_B(2))}_{\delta b_2} + \sum_{m_1} \overline{p(\Omega_B(1))}_{\delta b_1}. \tag{28}$$

We note that in Eq. (27) neither the coefficient $\langle P\rangle$ nor the function M do depend on the probe pulse frequency ω_A. Taking into account Eq. (22) we see that expression (26) has a Gaussian form with respect to the variable ω_A. The maximum of this curve is achieved at the frequency

$$\omega_A^{\text{max}} = \gamma_0 B_0 g_{\text{eff}}(0,0,\beta)/g_e + \gamma_0 A_{\text{eff}}(0,0,\beta). \tag{29}$$

This is the most important theoretical result of this work. The function u as well as the point ω_A^{max}, where it reaches its maximum value, can be determined experimentally. Following Eq. (29), the angle β characterizing the geometry of the spin labels attached to DNA can be determined.

IV. EXPERIMENTS

In this section we describe the application of the theoretical method developed above to experiments with double
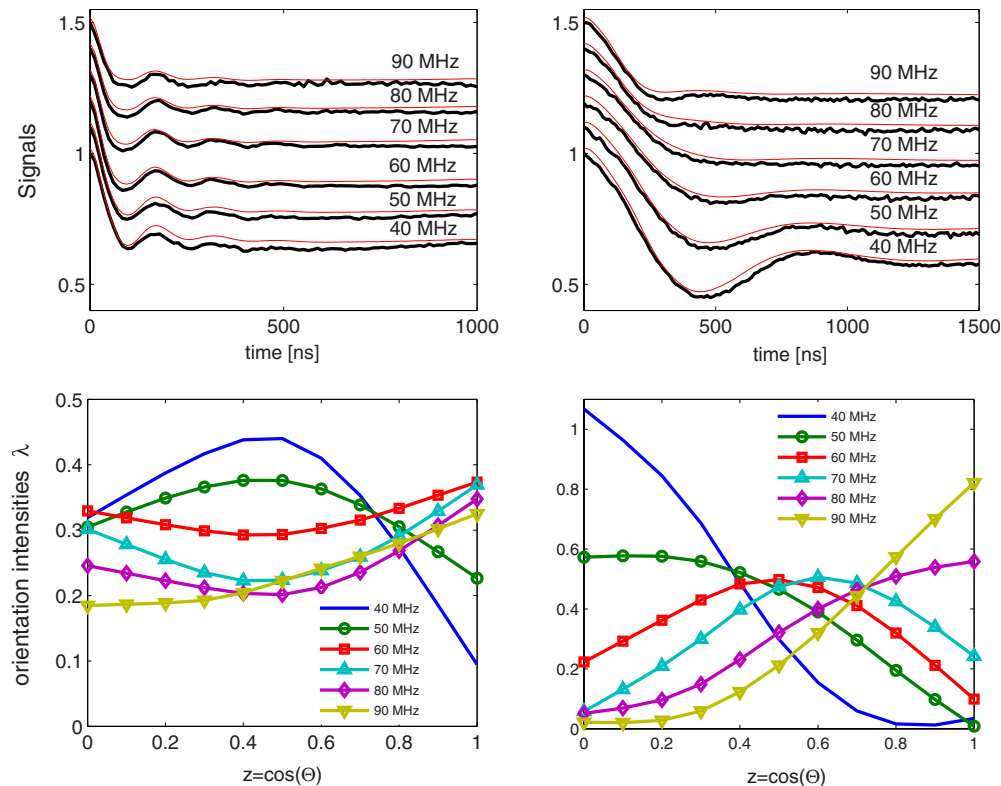
FIG. 4. (Color online) Analysis of the PELDOR experiments with double labeled DNA molecules: (left) DNA(1,5) and (right) DNA(1,12). (Top) Sets of six experimental time traces (bold black curves) obtained with the fixed pump pulse frequency and six different probe pulse frequencies ranging from 40 to 90 MHz with a step of 10 MHz. For a convenient presentation the curves are consecutively shifted 0.1 upwards. Reconstructed time traces (thin red curves) from intensity orientation functions. (Bottom) Orientation intensity functions obtained by Tikhonov regularization.

labeled DNA molecules. A detailed description of the synthesis of these molecules, in which a nitroxide group is incorporated into a polycyclic fused ring system of cytidine analog that forms a base pairs with guanine, has been described recently [28]. PELDOR measurements were performed for double helical DNA molecules with several different orientations of the spin label plane normals with respect to the interspin vector *r* (see Figs. 1 and 3). All measurements were performed in a frozen aqueous buffer solutions at a temperature of 40 K. The duration of the pump pulse was t_B =12 ns, centered at the resonance frequency ω_B =9.786 GHz of the dielectric microwave Bruker resonator. The frequency of the t_A=32 ns long probe pulses was gradually shifted from the resonator frequency in the range from 40 to 90 MHz in steps of 10 MHz. The excitation bandwidths of the pump and probe pulses were chosen small enough to avoid severe spectral overlap of the pulses even for the lowest detection frequency offset of $\Delta\nu$=40 MHz. On the other hand, the excitation width of the pump pulse should be as large as possible to achieve a deep modulation depth. In all ten investigated molecules the first spin label was fixed at the same position while the position of the second label was different in different samples. In terms of Fig. 1, this means that the first label was always attached at position 1 whereas the second label migrated from position 5 to 14. Figure 4 shows two examples of PELDOR time traces obtained from DNA(1,5) and DNA(1,12). Similar data were obtained for

other eight samples but are not shown here. For each sample a set of six PELDOR time traces for probe frequencies offsets ranging from 40 to 90 MHz have been recorded. The resulting signals were normalized to their maximal values at zero time, and the intermolecular exponential decay has been factored out.

The measured time traces can be used to find the orientation intensity functions from Eq. (5) if the interspin distance distribution necessary to calculate the kernel function $K(z,T)$ is known. Due to the short spectral width of the probe pulses in comparison to the whole nitroxide spectra, our experimental signals are strongly influenced by orientation selection effects. Thus, the direct determination of the distance distribution function from one time trace with the fixed probe and pump pulse frequencies can be inaccurate. To reduce the effects of noncomplete spectral excitation the PELDOR time traces recorded at different spectral positions were summed. Using the average over all offset frequencies as input data the distance distribution function has been determined by the DEER ANALYSIS program [33] disregarding possible orientation selection effects. Thus, the obtained kernel function and experimental PELDOR time traces can be inserted into Eq. (5) in order to find numerically the function $\lambda(z,\omega_A,\omega_B)$ for each frequency offset. A detailed analysis of the numerical solution with the application to model systems has been published recently [27]. To solve Eq. (5), we discretized the time T into L steps of length $\Delta T=T_{max}/L$ and the parameter z

$\in [0,1]$ into M steps of length $\Delta z = 1/M$. This allows us to represent Eq. (5) in matrix form as

$$s_i = \sum_j K_{ij}\lambda_j \quad \text{or} \quad \mathbf{s} = \hat{K}\boldsymbol{\lambda}, \tag{30}$$

where $s_i \equiv S(T_i, \nu) - 1$, $K_{ij} \equiv K(T_i, z_j)\Delta z$, and $\lambda_j = \lambda(z_j, \nu)$. Expression (30) constitutes an overdetermined system of linear equations, i.e., it represents an ill-posed problem whose solutions may be unstable. To solve Eq. (30), Tikhonov regularization [4,15–18] is used to minimize the functional

$$\left\| \mathbf{s}_{\text{exp}} - \hat{K}\boldsymbol{\lambda} \right\| + \alpha \left\| \frac{d^2\lambda(z)}{dz^2} \right\| \rightarrow \min. \tag{31}$$

Here, α is a regularization parameter that depends on the quality of the experimental data and determines the smoothness of the solution. The above expression is minimized when

$$\boldsymbol{\lambda} = \left| \hat{K}^T\hat{K} + \alpha \hat{D}^T\hat{D} \right|^{-1} \hat{K}^T \mathbf{s}_{\text{exp}}, \tag{32}$$

where $\hat{D}$ is the second derivative operator written in matrix representation. Inserting experimental time traces $\mathbf{s}_{\text{exp}}$ obtained from one sample, the last expression is used to calculate the orientation intensity function $\lambda(z, \omega_A, \omega_B)$ for different probe pulse frequencies ω_A. The value of the regularization parameter was taken equal to $\alpha = 50$ for all 60 analyzed PELDOR time traces. It was calculated setting the limit for the deviation of the fit curves from the experimental data equal to the averaged level of noise. The dependence of the solution on the regularization parameter was rather weak. Increasing or decreasing in α by a factor of five did not change the result of the estimation substantially. The results of these calculation are displayed on the Fig. 4. The orientation intensity functions for the DNA(1,12) demonstrate clear regions of high and low intensity, whereas for DNA(1,5) the function λ is relatively flat. This means that the orientation selection effects are more pronounced in the former case. As described in theoretical section the frequency dependence of the orientation intensity function for $\Theta = 0$ can be used for the determination of the nitroxide mutual orientation.

V. DISCUSSION AND CONCLUSIONS

On the one hand, according to Eq. (7), the function u is given for $\Theta = 0$ by the expression $\langle u(\omega_A, \omega_B, 0, \mathbf{o}_1^{(i)}, \mathbf{o}_2^{(i)}) \rangle = \lambda(1, \omega_A, \omega_B)V_0(\omega_A) \equiv \Lambda(\Delta\nu)$, where $V_0(\omega_A)$ can be determined from the nitroxide field sweep spectrum. The values of $\langle u(\omega_A, \omega_B, 0, \mathbf{o}_1^{(i)}, \mathbf{o}_2^{(i)}) \rangle$ extracted from the experimental data are shown on Fig. 5 as functions of the frequency offset between the probe and pump pulses, $\Delta\nu$, which is related to ω_A as $\omega_A = \omega_B + 2\pi\Delta\nu$. On the other hand, the function u is described by expression (27), which has a Gaussian form with respect to ω_A and consequently to $\Delta\nu$. Therefore, the obtained data have been fitted with a Gaussian curve for each sample (see Fig. 5). The curves that fit DNA(1,5) and DNA(1,12) achieve their maxima at $\Delta\nu_{(1,5)} = 64 \pm 1$ MHz and at $\Delta\nu_{(1,12)} = 81 \pm 1$ MHz, respectively. The determination of the Gaussian curves centers depends slightly on the data analysis procedure. Inaccuracies linked with the elimi-
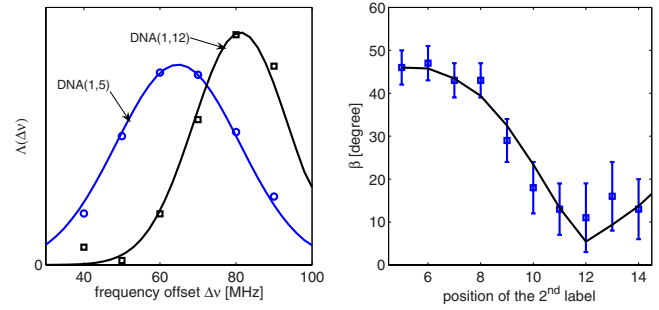
FIG. 5. (Color online) (Left) Estimated values of the function $\Lambda(\Delta\nu) \equiv \lambda(1, \omega_A, \omega_B)V_0(\omega_A)$ for DNA(1,5)—circles and DNA(1,12)—rectangles. Both estimations are fitted with Gaussian curves. (Right) Estimated values of the angle between spin label normals and interspin vector $\mathbf{r}$ versus the position of the second spin label compared to the values of these angles obtained from DNA structure (solid line).

nation of the intermolecular relaxation, the determination of the $T = 0$ point of the time traces and the choice of the regularization parameter can lead to variations in the Gaussian center of up to 1 MHz. The obtained values of $\omega_A^{\max}$ can be inserted into Eq. (29), which explicitly can be written in the following form:

$$\frac{\omega_A^{\max}}{\gamma_0} = \frac{B_0}{g_e}\sqrt{g_{xx}^2 + (g_{zz}^2 - g_{xx}^2)\cos^2\beta} + \sqrt{A_{xx}^2 + (A_{zz}^2 - A_{xx}^2)\cos^2\beta}. \tag{33}$$

In the last expression the magnetic field value $B_0 = 3470$ G corresponds to the point where nitroxide field sweep spectrum recorded at the pump pulse frequency $\omega_B = 9.786$ GHz reaches its maximum. Employing the g-tensor values $g_{xx} = 2.0075$, $g_{yy} = 2.0075$, $g_{zz} = 2.0025$, and hyperfine interaction tensor values $A_{xx} = 5$ G, $A_{yy} = 5$ G, and $A_{zz} = 35$ G, we obtained angles $\beta_{(1,5)} = 46° \pm 4°$ and $\beta_{(1,12)} = 11° \pm 8°$. Generally, the solution of Eq. (33) yields angles β close to $0°$ if the frequency $\omega_A^{\max}$ lies at the edge of the nitroxide spectrum and large β close to $90°$ if $\omega_A^{\max}$ is near the center of nitroxide spectrum. The estimation error of the angle β is caused by the inaccuracy in the determination of the frequency $\omega_A^{\max}$, as mentioned above. Due to uncertainty propagation the errors are larger for the small angles β than for large ones.

A similar estimation procedure has been performed for the samples with the labels attached to other positions within DNA molecule. The obtained results for the angles between nitroxide normals and interspin vector have been compared to the values of these angles obtained from DNA structure. A fairly good agreement of both results is observed (see Fig. 5 right panel). At this point it is relevant to recall our previous work [27], where a linear biradical model system with predominantly perpendicular orientation of the A_{zz} axes with respect to interpin axis $\mathbf{r}$ have been studied using orientation intensity functions. For these system the behavior of the function $\Lambda(\Delta\nu)$ demonstrate an opposite trend compared to those of DNA(1,12). In contrast to DNA(1,12), where $\Lambda(\Delta\nu)$ increases when the frequency gap between the probe and pump pulses growths, for the linear biradical the function

$\Lambda(\Delta\nu)$ increases when the frequency gap becomes smaller. It reaches its maximum at the point $\Delta\nu^{max} < 40$ MHz that is smaller than the smallest frequency gap used in the experiments. Nevertheless, we can employ Eq. (33) to estimate angle β between nitroxide normals and r. The estimation yields $\beta > 76°$, that is in a good agreement with considered geometry of the linear biradical.

Besides the angle β that is assumed to be the central value of normally distributed angles β_1 and β_2, the geometry of biradical is characterized by other Euler angles α_2, γ_1, and γ_2 (see Fig. 3). In principal, determination of α_2 from X-band data is possible by performing fitting procedure of PELDOR time traces. However, it was not possible to derive an expression similar to Eq. (33) for α_2 yet. Because at X-band frequencies the EPR spectrum is dominated by axial A tensor, it is more difficult to track the angles γ_1 and γ_2 in PELDOR experiments. The nitroxide rotation around its normal or variation in the angle γ_1 or γ_2 does not change radical resonance frequency value [see Eqs. (14) and (15)] and consequently the time traces are also not changed. For the determination of γ_1 and γ_2, high-field measurement would be required, where the orientation of g-tensor principal axis is spectrally resolved.

To conclude, the influence of the mutual nitroxide orientation on the PELDOR time traces as well as the solution of the inverse problem have been studied. We have shown how for the specific case of a symmetry related pair of nitroxide radicals the angle between the nitroxide plane normal and the interconnecting vector r could be directly determined via an analytical expression from PELDOR time traces taken with variable probe frequencies. On a double stranded DNA molecule with rigidly attached spin labels, it was shown that the angles found in that manner are in good agreement with expectations. Determination of the spin labels mutual orientation can be employed for the studies of DNA molecule structural changes under the influence of physical and chemical factors [14,34–37].

[1] A. D. Milov, K. M. Salikhov, and J. E. Shirov, Fiz. Tverd. Tela (Leningrad) **23**, 975 (1981).

[2] A. D. Milov, A. B. Ponomarev, and Y. D. Tsvetkov, Chem. Phys. Lett. **60**, 4508 (1984).

[3] A. Schweiger and G. Jeschke, *Principles of Pulsed Electron Paramegnetic Resonance* (Oxford University Press, Oxford, 2001).

[4] G. Jeschke and Y. Polyhach, Phys. Chem. Chem. Phys. **9**, 1895 (2007).

[5] O. Schiemann and T. Prisner, Q. Rev. Biophys. **40**, 1 (2007).

[6] J. R. Lakowicz, *Principles of Fluorescence Spectroscopy* (Plenum, New York, 1999).

[7] O. Schiemann, N. Piton, Y. Mu, G. Stock, J. Engels, and T. F. Prisner, J. Am. Chem. Soc. **126**, 5722 (2004).

[8] N. Piton, Y. Mu, G. Stock, T. Prisner, O. Schiemann, and J. Engels, Nucleic Acids Res. **35**, 3128 (2007).

[9] O. Schiemann, N. Piton, J. Plackmeyer, B. Bode, T. Prisner, and J. Engels, Nat. Protoc. **2**, 904 (2007).

[10] N. Barhate, P. Cekan, A. P. Massey, and S. T. Sigurdsson, Angew. Chem., Int. Ed. **46**, 2655 (2007).

[11] T. E. Edwards and S. T. Sigurdsson, Nat. Protoc. **2**, 1954 (2007).

[12] Q. Cai, A. K. Kusnetzow, W. L. Hubell, I. S. Haworth, G. P. C. Gacho, N. Eps, K. Hideg, E. J. Chambers, and P. Z. Qin, Nucleic Acids Res. **34**, 4722 (2006).

[13] M. Persson, J. R. Harbridge, P. Hammastrom, R. Mitri, L. Martensson, U. Carlsson, G. R. Eaton, and S. S. Eaton, Biophys. J. **80**, 2886 (2001).

[14] G. Sicoli, G. Mathis, O. Delalande, Y. Boulard, D. Gasparutto, and S. Gambarelli, Angew. Chem., Int. Ed. **47**, 735 (2008).

[15] Y. Chiang, P. Borbat, and J. Freed, J. Magn. Reson. **172**, 279 (2005).

[16] Y. Chiang, P. Borbat, and J. Freed, J. Magn. Reson. **177**, 184 (2005).

[17] G. Jeschke, G. Panek, A. Godt, A. Bender, and H. Paulsen, J. Magn. Reson. **169**, 1 (2004).

[18] G. Jeschke, G. Panek, A. Godt, A. Bender, and H. Paulsen, Appl. Magn. Reson. **26**, 223 (2004).

[19] A. G. Maryasov, Y. D. Tsvetkov, and J. Raap, Appl. Magn. Reson. **14**, 101 (1998).

[20] A. D. Milov, A. G. Maryasov, and Y. D. Tsvetkov, Appl. Magn. Reson. **15**, 107 (1998).

[21] R. G. Larsen and D. J. Singel, J. Chem. Phys. **98**, 5134 (1993).

[22] V. Denysenkov, T. F. Prisner, J. Stubbe, and M. Bennati, Proc. Natl. Acad. Sci. U.S.A. **103**, 13386 (2006).

[23] A. Savitsky, A. A. Dubinskii, W. Lubitz, and K. Möbius, J. Phys. Chem. B **111**, 6245 (2007).

[24] V. Denysenkov, D. Biglino, W. Lubitz, T. Prisner, and M. Bennati, Angew. Chem., Int. Ed. **47**, 1224 (2008).

[25] Y. Polyhach, A. Godt, C. Bauer, and G. Jeschke, J. Magn. Reson. **185**, 118 (2007).

[26] D. Margraf, B. Bode, A. Marko, O. Schiemann, and T. Prisner, Mol. Phys. **105**, 2153 (2007).

[27] A. Marko, D. Margraf, H. Yu, Y. Mu, G. Stock, and T. Prisner, J. Chem. Phys. **130**, 064102 (2009).

[28] O. Schiemann, P. Cekan, D. Margraf, T. Prisner, and S. T. Sigurdsson, Angew. Chem. **48**, 3292 (2009).

[29] P. Cekan, A. L. Smith, N. Barhate, B. H. Robinson, and S. T. Sigurdsson, Nucleic Acids Res. **36**, 5946 (2008).

[30] M. Pannier, S. Viet, A. Godt, G. Jeschke, and H. W. Spiess, J.

Magn. Reson. **142**, 331 (2000).

[31] A. Marko, B. Wolter, and W. Arnold, Phys. Rev. B **69**, 184424 (2004).

[32] A. Marko, B. Wolter, and W. Arnold, J. Magn. Reson. **185**, 19 (2007).

[33] G. Jeschke, V. Chechik, P. Ionita, A. Godt, H. Zimmermann, J. Banham, C. R. Timmel, D. Hilger, and H. Jung, Appl. Magn. Reson. **30**, 473 (2006).

[34] N. A. Kuznetsov, A. D. Milov, V. V. Koval, R. I. Samoilova, Y.

A. Grishin, D. G. Knorre, Y. D. Tsvetkov, O. S. Fedorova, and S. A. Dzuba, Phys. Chem. Chem. Phys. **11**, 6826 (2009).

[35] G. Sicoli, G. Mathis, S. Aci-Seche, C. Saint-Pierre, Y. Boulard, D. Gasparutto, and S. Gambarelli, Nucleic Acids Res. **37**, 3165 (2009).

[36] A. K. Mazur, Phys. Rev. E **80**, 010901(R) (2009).

[37] R. S. Mathew-Fenn, R. Das, and P. A. B. Harbury, Science **322**, 446 (2008).